GLOBAL BIOGEOCHEMICAL CYCLES, VOL. 14, NO. 4, PAGES 1299-1313, DECEMBER 2000

Estimating the convective supply of nitrate and implied variability in export production over the North Atlantic

Richard G. Williams and Alison J. McLaren
Oceanography Laboratories, Department of Earth Sciences, University of Liverpool, Liverpool, England, United Kingdom

Michael J. Follows
Program in Atmospheres, Oceans and Climate, Massachusetts Institute of Technology, Cambridge

Abstract. The maintenance and interannual variability of export production is partly controlled by the convective and Ekman supply of nutrients to the euphotic zone. This dynamical supply of nitrate to the euphotic zone is estimated over the North Atlantic from 1968 to 1993. First, a matrix of one-dimensional mixed-layer models are integrated over the North Atlantic forced by surface and Ekman fluxes of heat and freshwater. Second, nitrate fluxes to the euphotic zone are estimated by combining the mixed-layer thickness cycle and wind stress data with climatological nitrate profiles. The model suggests that the convective supply of nitrate ranges from 0.1 mol N $m^{-2}yr^{-1}$ in the subtropics to 1.4 mol N $m^{-2}yr^{-1}$ over the subpolar gyre. The interannual variability in convective supply reaches ± 0.2 mol N $m^{-2}yr^{-1}$. This variability in nitrate supply is significantly correlated with the North Atlantic Oscillation index over parts of the central and western Atlantic but not over the eastern Atlantic. This convectively induced variability should modulate the levels of export production wherever the nitrate supply is limiting. The Ekman transfer is relatively small, reaching 0.1 mol N $m^{-2}yr^{-1}$ over the subpolar gyre, but is important in maintaining nitrate concentrations within the seasonal boundary layer.

1. Introduction

Export production, defined by the loss of organic matter from the euphotic zone, is maintained both through physical processes which transfer nutrients within the ocean and external inputs of nutrients from the atmosphere and land (Figure 1a). The basin-scale patterns in export production over the North Atlantic broadly reflect the combined effects of convection and circulation in transferring nutrients (Figure 1b).

For example, remotely sensed estimates of primary production [*Sathyendranath et al.,* 1995; *Behrenfeld and Falkowski,* 1997] indicate more vigorous productivity over the subpolar gyre, tropics and coastal boundaries, which are consistent with high export fluxes as implied from sediment-trap measurements [*Lampitt and Antia,* 1997]. In these productive regions, convection and large-scale upwelling combine to transfer nutrient-rich, thermocline waters into the euphotic zone. Over the subpolar gyre, this vertical supply of nutrients is enhanced by the lateral transfer of thermocline waters into the poleward deepening, winter mixed layer [*Marshall et al.*, 1993]. Primary production and perhaps export production is weaker over the subtropical gyre where there is large-scale downwelling. Over the flanks of the subtropical gyre, export production is probably maintained through a combination of convection and a lateral, wind-driven transfer of nutrients from neighboring upwelling zones [*Williams and Follows*, 1998]. However, independent, transient-tracer estimates of export production over the Sargasso Sea [*Jenkins*, 1982, 1988; *Jenkins and Goldman*, 1995] are only partly explained by traditional sources of nitrogen involving convection [*Michaels et al.*, 1994], diapycnic diffusion [*Lewis et al.*, 1986], and atmospheric deposition [*Knap et al.*, 1986]. Instead, additional nitrogen sources have been proposed involving rectified eddy-induced upwelling of nutrients [*McGillicuddy and Robinson*, 1997], a lateral transfer of organic nutrients [*Rintoul and Wunsch,* 1991], and nitrogen fixation [*Michaels et al.,* 1996; *Gruber and Sarmiento,* 1997].

While a steady-state view is a useful starting point to understand patterns of export production, there is

Paper number 2000GB001260.
0886-6236/00/2000GB001260$12.00

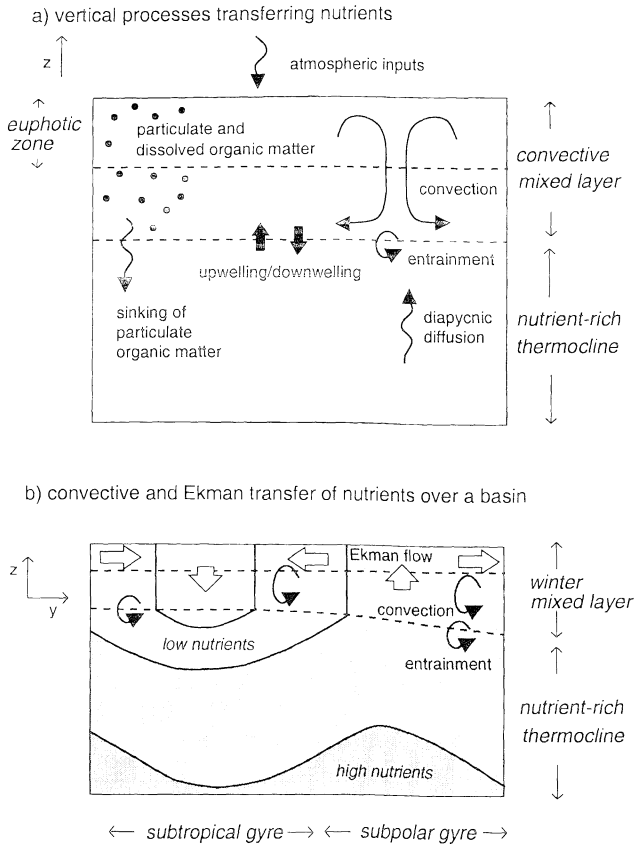

Figure 1. (a) Export production involves an export of organic matter from the euphotic zone. This process is maintained through a combination of external inputs of nutrients and physical processes supplying nutrients from the thermocline. The bases of the euphotic zone and mixed layer are marked here by the upper and lower dashed lines, respectively. (b) The physical supply of nutrients varies over the basin due to the poleward increase in convection and the gyre-scale variations in the wind-driven circulation; the seasonal boundary layer is defined by the thickness of the end of winter mixed layer (marked by the dashed line).

strong interannual variability over the upper ocean of the North Atlantic involving both physical and biogeochemical variables. Interannual changes in sea surface temperature (SST) are associated with atmospheric anomalies and changes in air-sea fluxes [*Bjerknes*, 1964; *Kushnir*, 1994; *Cayan*, 1992a]. *Cayan* [1992b] argued that the atmospheric anomalies drive the SST changes on interannual timescales, since the tendency in SST correlates with latent and sensible heat flux anomalies. This interpretation is supported by *Battisti et al.* [1995], who successfully simulated wintertime variations in SST (away from the Gulf Stream) over the North Atlantic only using air-sea fluxes (and without including any anomalous advection of SST). The atmospheric anomalies also alter the strength and pattern of oceanic convection over the North Atlantic [*Dickson et al.*, 1996] as well as modifying the circulation.

In turn, the meteorologically forced interannual changes in convection and circulation modulate the nutrient supply to the euphotic zone and thus alter export production in regions limited by macronutrients. For example, local winter mixing has been found to alter primary production in the Sargasso Sea [*Menzel and Ryther*, 1961] and to influence the interannual variability of the modeled particulate export at Hydrostation S, near Bermuda [*Steel and Henderson*, 1993]. In addition, biogeochemical modeling and remote ocean color studies of the North Atlantic show interannual changes in convection controlling both spring-time phytoplankton abundance [*Dutkiewicz et al.*, 2000; M.J. Follows and S. Dutkiewicz, Meteorological modulation of the North Atlantic spring bloom, submitted to *Deep Sea Research*, 2000] and air-sea exchange of gases [*McKinley et al.*, 2000].

In this study, we adopt a simplified modeling approach in order to estimate the convective and wind-induced (Ekman) supply of nitrate to the euphotic zone over the North Atlantic for a 26-year period from 1968 to 1993. A matrix of one-dimensional, mixed-layer models is used to estimate changes in mixed-layer thickness over the North Atlantic forced by air-sea fluxes; this approach is similar to that adopted by *Battisti et al.* [1995]. The convective and Ekman transfer of nitrate to the euphotic zone is estimated by melding the modeled mixed-layer thickness changes with climatological nitrate profiles.

In section 2, the convective supply of nutrients to the euphotic zone is discussed in terms of its contribution to export production. In section 3, a one-dimensional mixed-layer model is developed and tested by comparing with observations at the Bermuda Atlantic Time-Series Study (BATS). In section 4, the one-dimensional model is used to estimate the convective and Ekman supply of nitrate to the euphotic zone over the North Atlantic using time series for surface fluxes of heat and freshwater, and wind stress, combined with climatological nitrate profiles. This dynamical supply of nitrate is correlated with changes in the North Atlantic Oscillation (henceforth referred to as NAO). Finally, the results are discussed in section 5.

2. Convective Nutrient Supply and Export Production

The local evolution of a dissolved inorganic nutrient, $\mathcal{N}$, is controlled by the divergence of the advective fluxes, $\nabla\cdot(\mathbf{u}\mathcal{N})$, the vertical divergence of the turbulent fluxes, $\frac{\partial}{\partial z}\overline{w'\mathcal{N}'}$, and biological cycling, $\partial F/\partial z$:

$$\frac{\partial \mathcal{N}}{\partial t} + \nabla\cdot(\mathbf{u}\mathcal{N}) + \frac{\partial}{\partial z}\overline{w'\mathcal{N}'} = \frac{\partial F}{\partial z}, \qquad (1)$$

where $\mathbf{u}$ is the three-dimensional velocity vector, w is the vertical velocity, $\overline{w'\mathcal{N}'}$ represents a vertical tur-

bulent nutrient flux, the prime represents a turbulent event in the mixed layer, and the overline represents a time average of these turbulent events. Geostrophic eddy transport and mixing is included in the term $\nabla \cdot (\mathbf{u}\mathcal{N})$. The biological sources and sinks of inorganic nutrients are simply represented by the convergence of the downward flux of particulate and dissolved organic matter, F. Export production is defined here as the flux of organic matter out of the euphotic zone, $F(-h_e)$, which includes the sinking of particulate organic matter and the advection and turbulent mixing of dissolved organic matter. The export production is related to the nutrient supply by integrating (1) over the euphotic zone of thickness h_e:

$$h_e \frac{\partial \mathcal{N}_m}{\partial t} + \int_{-h_e}^{0} \nabla \cdot (\mathbf{u}\mathcal{N}) dz + \overline{w'\mathcal{N}'}_{z=0} - \overline{w'\mathcal{N}'}_{z=-h_e} = -F(-h_e), \quad (2a)$$

where the subscript m denotes a value in the mixed layer and the surface flux of organic nutrients is neglected. The export production, $F(-h_e)$, is driven by the temporal change in nutrient concentration in the euphotic zone, advective supply of nutrients, surface input of nutrients, or the convective supply of nutrient-rich water (represented by the first to fourth terms on the left-hand side of (2a), respectively).

On a seasonal timescale, this nutrient balance over the euphotic zone (see the scale analysis in the Appendix of *Williams and Follows* [1998]) reduces to

$$h_e \frac{\partial \mathcal{N}_m}{\partial t} - \overline{w'\mathcal{N}'}_{z=-h_e} = -F(-h_e), \quad (2b)$$

where mixed-layer nutrients decrease in concentration through biological consumption and export during spring and summer and increase again through convective supply during autumn and winter. For a steady state, the convective supply of nutrients approximately balances the export production over the year:

$$\int_{\text{year}} \overline{w'\mathcal{N}'}_{z=-h_e} dt = \int_{\text{year}} F(-h_e) dt. \quad (3)$$

Hence we attempt here to estimate the convective supply of nutrients each winter in order to estimate export production over the following year.

The dominant nutrient balance differs from (2b) when integrated over the seasonal boundary layer as discussed by *Williams and Follows* [1998], since the entrainment flux, $\overline{w'\mathcal{N}'}$, becomes much smaller at the base of the seasonal boundary layer. The depth-integrated nutrients over the seasonal boundary layer are instead maintained by the combination of convection, advective fluxes, and surface nutrient inputs.

We now develop a simplified mixed-layer model to estimate the convective and Ekman supply of nitrate in order to diagnose their contributions to export production. The model is first tested at BATS (section 3) and then applied over the North Atlantic (section 4).

3. A Mixed-Layer Model Applied in the Sargasso Sea

3.1. One-Dimensional Mixed-Layer Model

A one-dimensional, *Kraus and Turner* [1967] style, mixed-layer model is used to solve the density and turbulent kinetic equations on seasonal timescales, which includes parameterized heat and freshwater advection to obtain a closed annual cycle; further details are given by *Williams* [1988] and *Lascaratos et al.* [1993]. The density budget for the mixed layer involves a balance between local temporal change, advection of density, surface fluxes, and entrainment:

$$h \frac{\partial \rho_m}{\partial t} + \int_{-h}^{0} \nabla \cdot (\mathbf{u}\rho) dz = -\frac{\alpha}{C_p} \mathcal{H} + \overline{w'\rho'}_{z=-h}, \quad (4)$$

where, for clarity, we do not include surface fresh water fluxes or penetrating solar radiation in (4) but do include these terms in the subsequent model integrations; h is the mixed-layer thickness, ρ_m is the mixed-layer density, $\mathcal{H}$ is the surface heat flux, $\overline{w'\rho'}_{z=-h}$ is the turbulent density flux at the base of the mixed layer, α is the density expansion coefficient for temperature, and C_p is the heat capacity.

The mixed-layer density budget is controlled by surface forcing and entrainment over seasonal timescales, but advection becomes important on an annual timescale. Our objective is to develop a mixed-layer model that can be applied over different parts of the basin by including a parameterized advection; our approach has been applied in the eastern Mediterranean [*Lascaratos et al.*, 1993] and is similar to that used by *Battisti et al.* [1995] for the North Atlantic.

First, the advection is separated into contributions from the geostrophic velocity $\mathbf{u}_g$ and the horizontal Ekman volume flux $\mathbf{U}_{ek}$, and (4) is rewritten as

$$h \frac{\partial \rho_m}{\partial t} + \int_{-h}^{0} \nabla \cdot (\mathbf{u}_g \rho) dz + \mathbf{U}_{ek} \cdot \nabla_h \rho_m = -\frac{\alpha}{C_p} \mathcal{H} + \overline{w'\rho'}_{z=-h}, \quad (5)$$

where ∇_h represents a horizontal derivative.

Second, we assume that the interannual changes in surface and Ekman fluxes are larger than those in geostrophic advection; this assumption is supported by the studies of *Cayan* [1992b] and *Battisti et al.* [1995]. The climatological-mean contribution from geostrophic advection must be parameterized. If there is a nearly repeating annual cycle, time-averaging (5) and integrating over the seasonal boundary layer of thickness H (de-

fined by the maximum thickness of the winter mixed-layer) gives

$$\int_{-H}^{0} \nabla \cdot (\overline{\mathbf{u}_g \rho}^c) dz = -\frac{\alpha}{C_p} \overline{\mathcal{H}}^c - \overline{\mathbf{U}_{ek} \cdot \nabla_h \rho_m}^c, \quad (6)$$

where the temporal change, first term in (5), is neglected by assuming a nearly steady state, the entrained density flux, $\overline{w'\rho'}_{z=-H}$, at the base of the climatological, seasonal boundary layer is assumed to be relatively small, and the overline with superscript c represents a climatological-annual average.

Here, we choose to parameterize the vertically integrated, geostrophic advection of density into the seasonal boundary layer using (6) in terms of the residual of the time-averaged surface density and Ekman fluxes. The contribution from geostrophic advection is only included over the climatological seasonal boundary layer. The advective flux is assumed to decay exponentially with depth with an e-folding depth scale equal to half the thickness of the climatological end of winter mixed-layer. Note that *Battisti et al.* [1995] also includes an additional heat flux in order to obtain a closed heat balance but instead applies this flux only at the surface. Our advective parameterization supplying additional heat and freshwater over the seasonal boundary layer leads to an improved seasonal cycle in the upper thermocline; for example, the model correctly simulates the summer formation of a subsurface salinity minimum over the eastern Mediterranean [*Lascaratos et al.*, 1993], which is not possible to obtain with only surface forcing.

The mixed-layer thickness and density are solved for from the density budget (equation (5)) and the turbulent kinetic energy equation of the mixed-layer model [*Williams*, 1988] using surface density fluxes and winds, together with the parameterization for the geostrophic advection (equation (6)). The mixed-layer model and advective parameterization is extended to include penetrating solar radiation and surface freshwater fluxes.

3.2. Mixed-Layer Thickness Cycle at BATS

The mixed-layer model is first assessed at BATS (31°45'N, 64°10'W) for the period from 1989 to 1995 where there are in situ observations [*Michaels and Knap*, 1996]; note that there has been a detailed mixed-layer modeling study at that site by *Doney* [1996] from 1988 to 1992. The one-dimensional, mixed-layer model is

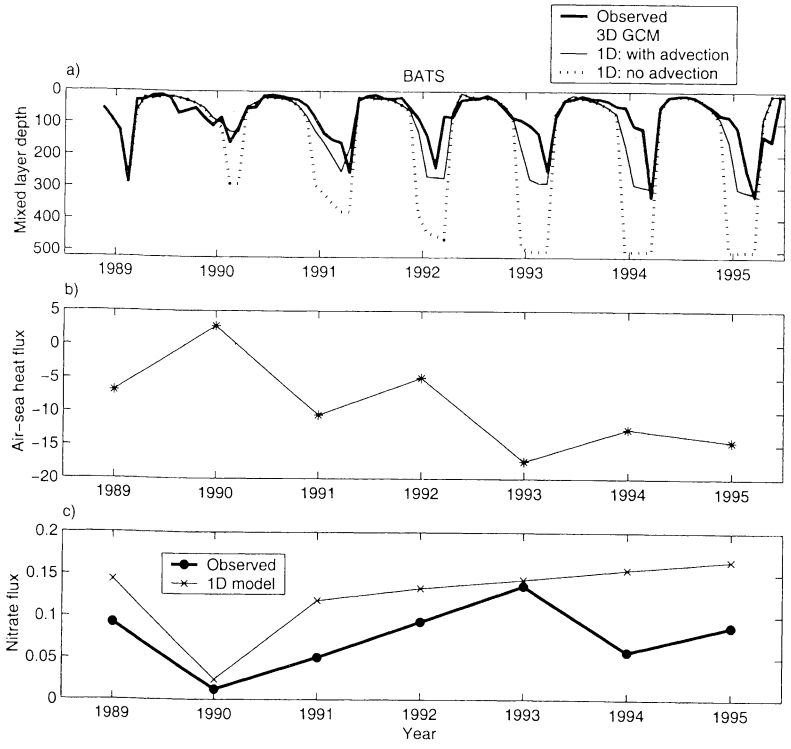

Figure 1. (a) Export production involves an export of organic matter from the euphotic zone. This process is maintained through a combination of external inputs of nutrients and physical processes supplying nutrients from the thermocline. The bases of the euphotic zone and mixed layer are marked here by the upper and lower dashed lines, respectively. (b) The physical supply of nutrients varies over the basin due to the poleward increase in convection and the gyre-scale variations in the wind-driven circulation; the seasonal boundary layer is defined by the thickness of the end of winter mixed layer (marked by the dashed line).

integrated with and without the geostrophic advection parameterization and compared with a general circulation model, which explicitly includes the geostrophic advection contribution. The observed density profiles diagnosed from bottle data at BATS suggest that the mixed-layer thickness at the end of winter varies interannually from 159 m in 1990 to 324 m in 1995 (Figure 2a, thick black line); using a mixed-layer thickness defined by a density jump of 0.125 kg m^{-3} from the surface.

The mixed layer is modeled using the idealized one-dimensional mixed-layer model and a three-dimensional general circulation model (GCM) [*Dutkiewicz et al.*, 2000]. The GCM has been integrated at $1^o \times 1^o$ resolution over the North Atlantic over this period using twice-daily NCEP analyzed heat and freshwater fluxes and wind stresses [*Kalnay et al.*, 1996], as well as including an additional surface relaxation term for temperature. In order to assess the role of advection, the one-dimensional model is forced using the same monthly surface fluxes as the GCM including the artificial surface relaxation for temperature. The annual surface heat flux applied in the model varies from 3 W m^{-2} over 1990 to -15 W m^{-2} in 1993 as shown in Figure 2b (these annual averages are evaluated from July to June). Ekman heat and salinity fluxes are evaluated from NCEP monthly winds combined with monthly SST [*Reynolds and Smith*, 1994] and climatological monthly salinity [*Levitus et al.*, 1994].

The one-dimensional model monotonically deepens, unrealistically, when forced only by surface fluxes due to the overall long-term surface heat loss (Figure 2a, dotted line). The parameterized geostrophic advection of heat and freshwater is chosen to be 14 W m^{-2} and 0.4 m yr^{-1}, which offsets the integrated surface and Ekman heat and freshwater fluxes between 1989 and 1995. The advection is applied over the climatological seasonal boundary layer and decays exponentially with a depth scale of 130 m. When the parameterized advection is included, the one-dimensional model gives much improved results, with the modeled variability broadly following observed changes and estimating a thickness of 128 m in 1990 and 318 m in 1995 (Figure 2a, thin full line). The correlation coefficient between the end of winter mixed-layer thickness from the one-dimensional model and the observations is 0.905, which is significant at a confidence level of 99%.

The GCM results are broadly similar to the one-dimensional model with parameterized advection showing only slightly improved agreement with the observed time series. Hence, the mixed-layer variability at BATS appears to be controlled by the integrated heat loss to the atmosphere, rather than interannual changes in geostrophic advection.

In comparison, *Doney* [1996] found that a one-dimensional, mixed-layer model reproduced much of the observed behavior in sea surface temperature, heat content, and mixed-layer thickness at BATS between 1988 and 1992. However, he argued that there was a poor representation of the end of winter mixed layer due to the omission of mesoscale features passing through the region. This omission is important for a detailed forecast at a specific site but may be less crucial on the basin scale.

3.3. Convective Nitrate Supply at BATS

The nitrate concentration in the mixed layer is inferred by combining the mixed-layer thickness and nitrate profiles using the integral method of *Glover and Brewer* [1988]. The annual entrainment flux of nitrate into the base of the euphotic zone is evaluated from monthly contributions from September until the end of winter:

$$\frac{1}{\mathcal{T}} \int_{\text{Sept}}^{W} \overline{w' \mathrm{NO}_3^{-\prime}}_{z=-h_e} dt, \tag{7}$$

where the end of winter, W, is defined to be when the surface heat flux changes from negative to positive and $\mathcal{T}$ represents 1 year, and the thickness of the euphotic zone is assumed always to be 100 m.

The entrainment flux into the euphotic zone in (7) is linearly related to the flux at the base of the mixed layer whenever the mixed layer is deeper than the euphotic zone and otherwise is zero:

$$\overline{w' \mathrm{NO}_3^{-\prime}}_{z=-h_e} = \Lambda_e \frac{h_e}{h} \overline{w' \mathrm{NO}_3^{-\prime}}_{z=-h}, \tag{8}$$

where $\Lambda_e = 1$ when $h \geq h_e$ and otherwise is 0. The entrainment flux at the base of the mixed layer is parameterized in terms of the mixed-layer deepening and nitrate difference between the mixed layer and underlying thermocline:

$$\overline{w' \mathrm{NO}_3^{-\prime}}_{z=-h} = \Lambda (\mathrm{NO}_{3\,th}^{-} - \mathrm{NO}_{3\,m}^{-}) \frac{\partial h}{\partial t}, \tag{9}$$

where $\mathrm{NO}_{3\,th}^{-}$ is the nitrate concentration in the fluid entrained from the thermocline and Λ is defined as 1 when there is entrainment with $\partial h/\partial t > 0$ and otherwise is 0.

The convective nitrate flux is determined at BATS from (7) to (9) using two independent methods. First, using the observed hydrography and monthly in situ nitrate profiles, the convective supply is estimated to reach 0.1 mol N $m^{-2}yr^{-1}$(Figure 2c, thick full line). This data-derived estimate varies from a minimum of 0.01 mol N $m^{-2}yr^{-1}$ in 1990 to 0.14 mol N $m^{-2}yr^{-1}$ in 1993. Second, the mixed-layer thickness is modeled and combined with the climatological-average of in situ nitrate profiles at BATS. The model-derived estimate is generally close to the data-derived estimate with values reaching 0.02 mol N $m^{-2}yr^{-1}$ in 1990 and 0.15 mol N $m^{-2}yr^{-1}$ in 1995 (Figure 2c, thin full line). The

modeled and observed convective fluxes do significantly differ in 1994 when observed nitrate profiles show low concentrations in the upper water column, which has been attributed to anomalous advection [*Michaels and Knap*, 1996].

Our estimates of the convective nitrate flux over the winter are similar in magnitude to estimates of new production of 0.09 mol N m^{-2} and 0.11 mol N m^{-2} for a spring bloom in 1989 by *Michaels et al.* [1994] (using oxygen excess and nitrate reduction methods, respectively). However, independent transient tracer evidence suggests that export production reaches higher values of typically 0.5 mol N $m^{-2}yr^{-1}$ over the Sargasso Sea [*Jenkins*, 1982, 1988; *Jenkins and Goldman*, 1985]. These higher values of export production are probably maintained by other nutrient sources becoming important (Figure 1a), such as fixation of nitrogen gas [*Michaels et al.*, 1996; *Gruber and Sarmiento*, 1997], mesoscale eddy transport [*McGillicuddy and Robinson*, 1997; *Oschlies and Garcon*, 1998], and lateral transport of organic matter [*Rintoul and Wunsch*, 1991]; see the review by *McGillicuddy et al.* [1998].

4. Interannual Change Over the North Atlantic

4.1. Model Formulation

We now employ the one-dimensional model in order to examine the convective and Ekman transfer of nitrate over the North Atlantic basin. Our approach assumes that interannual changes in the mixed layer over the basin scale are principally driven by interannual changes in air-sea fluxes. The model is integrated for separate stations at intervals of 1^o in latitude and longitude over the basin north of 20°N, in a similar manner to that employed by *Battisti et al.* [1995].

The surface solar heat flux is evaluated using astronomical relations and using monthly values of cloud cover [*da Silva et al.*, 1994] and climatological monthly albedo [*Payne*, 1972]. The solar irradiance is applied throughout the water column using an empirical, three exponential profile [*Horch et al.*, 1983], defined according to ocean color following a map of Sechi disc measurements over the North Atlantic [*Dickson*, 1972].

Monthly latent heat, sensible heat, longwave, precipitation fluxes and wind stress are taken from National Centers for Environmental Prediction (NCEP) [*Kalnay et al.*, 1996]. The Ekman fluxes of heat and freshwater are evaluated using monthly sea surface temperature [*da Silva et al.*, 1994] and climatological monthly salinity [*Levitus et al.*, 1994]. The model is initialized with climatological Levitus data in 1958 and integrated for 35 years: the first 10 years are considered as a spin up and the output is analyzed from 1968 to 1993.

The convective flux of nitrate is evaluated by combining the modeled cycle of mixed-layer thickness with climatological nitrate profiles [*Conkright et al.*, 1994]. The Ekman nitrate flux is evaluated by combining the time series of wind stress and the modeled mixed-layer nitrate concentrations. The resulting physical supply of nitrate to the euphotic zone provides an initial estimate of how much new and export production occurs over the following spring and summer assuming the simplified balance in (3). New and export production might be enhanced over our estimates owing to the contribution of other processes, such as atmospheric sources of nutrients, geostrophic eddy transport, and the transport of organic nutrients.

4.2. Model Test at Hydrostation S

We illustrate the performance of the array of one-dimensional models by a long-term comparison between the model and observed data at Hydrostation S in the Sargasso Sea (32°10'N, 64°30'W) [*Michaels and Knap*, 1996]. The annual surface and Ekman heat flux varies from -45 W m^{-2} in 1969 to 3 W m^{-2} in 1989 and is shown in Figure 3a together with its 10-year running average. The 10-year running mean reveals an overall surface cooling of -25 W m^{-2} in 1968 reducing to -2 W m^{-2} in 1993. The interannual variations in surface heat flux dominate over the Ekman heat flux, which has a climatological mean of -2 W m^{-2} here.

The mixed-layer thickness is predicted using the mixed-layer model with the parameterized geostrophic advection evaluated either from a 1- or 10-year running mean of the surface heat flux and the Ekman heat flux using (6). The interannual variability in the modeled field becomes unrealistically small when a 1-year running mean is used to evaluate the geostrophic advection, but becomes more plausible when a 10-year running mean is applied (Figure 3b). Henceforth, the geostrophic advection in the mixed-layer model is parameterized in terms of a 10-year running mean of the surface and Ekman density fluxes.

The observed and modeled variability in winter mixed-layer depth show some agreement for timescales of several years (there is a gap in the observed record in 1979 and 1980). The correlation coefficient between the observed and modeled variability is 0.44 for the annual fields and is significant at a level of 97.5%. When the modeled and observed time series' are smoothed over a timescale of 3 years (using a Gaussian filter) as shown in Figure 3c, the correlation coefficient rises slightly to 0.51 and is significant at a level of 99%. However, this value of the correlation coefficient suggests that the model only explains 26% of the variability. The model forecast exhibits less skill than at BATS, which might in part be due to increasing errors in the historical surface heat fluxes during this longer period of 26 years. In addition, the assumptions of the geostrophic heat balance parameterization are more uncertain on this longer timescale.

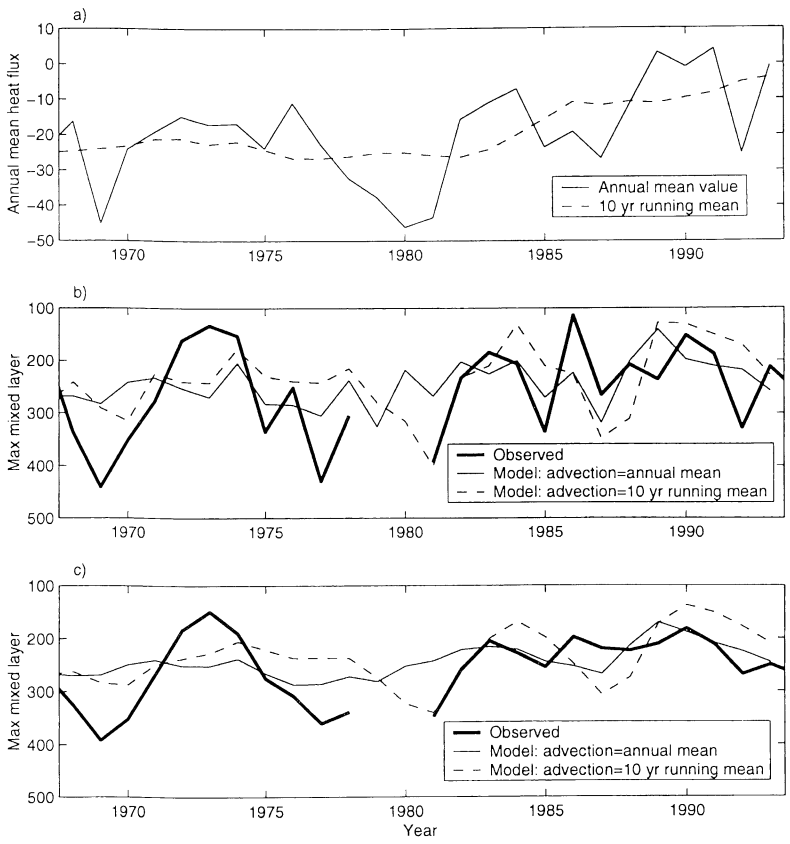

Figure 3. (a) Time-series of surface and Ekman heat flux (W m^{-2}) at Hydrostation S (solid line) and 10-year running mean (dashed line). (b) Mixed-layer thickness (m) at end of winter diagnosed from observations (thick solid line) and predicted from the one-dimensional mixed-layer model with geostrophic advection assumed to balance 1- or 10-year running mean of the surface heat flux (thin solid or dashed lines, respectively). (c) Smoothed version of Figure 3b over a 3-year timescale (using a Gaussian weighting).

4.3. Climatological Estimate of Convection

The model-derived, mixed layer is now examined over the North Atlantic, poleward of 20°N. The mixed-layer thickness in March, from an average of values between 1968 to 1993, is shown in Figure 4a. There is a tongue of a thicker mixed-layer extending to the northeast from 250 m at 35°N, 70°W to 500 m at 45°N, 20°W, and further thickening westwards along the northern rim of the subpolar gyre (Figure 4a). Mixed-layers of thickness greater than 150 m generally coincide with regions of net annual surface heat loss (derived from *da Silva et al.* [1994] and NCEP fluxes described in Section 4.1) (Figure 4b). The mixed-layer thickness is also diagnosed from climatology assuming a jump of 0.125 kg m^{-3} in potential density profiles, which are evaluated from temperature and salinity data [*Levitus and Boyer*, 1994; *Levitus et al.*, 1994]. The model-derived, winter mixed-layer topography is similar to that diagnosed from the Levitus climatology but is systematically slightly deeper (Figure 4c). However, our emphasis is assessing the interannual variability, which appears to be reasonably captured from the comparison at BATS. The standard deviation of the annual deviations in the thickness of the mixed layer in March varies from 25 m at low latitudes to greater than 150 m over the subpolar gyre (Figure 4d).

The convective flux of nitrate to the euphotic zone (defined by the upper 100 m) is evaluated using from the contributions between September to the end of winter for each year (equation (7)), from 1968 to 1993 is shown in Figure 5a. The annual convective supply broadly follows the pattern of the mixed-layer thickness with minimum values of 0.05 mol N $m^{-2}yr^{-1}$ at 25°N, 60°W and maximum values of 1.4 mol N $m^{-2}yr^{-1}$ in the subpolar gyre. There are zero convective fluxes where the mixed layer is thinner than 100 m located at 30°N, 40°W off Africa and Newfoundland. The standard deviation of the annual variations in the convective flux range from 0.05 to 0.2 mol N $m^{-2}yr^{-1}$ over this period from 1968 to 1993 (Figure 5b). This variability is comparable to the climatological mean nitrate supply at low latitudes but becomes an order of magnitude smaller than the mean supply at high latitudes. This reduced variability at

high latitudes is partly due to smaller relative changes in the mixed-layer thickness but also due to the weaker vertical nitrate gradient in the thermocline beneath the winter mixed layer.

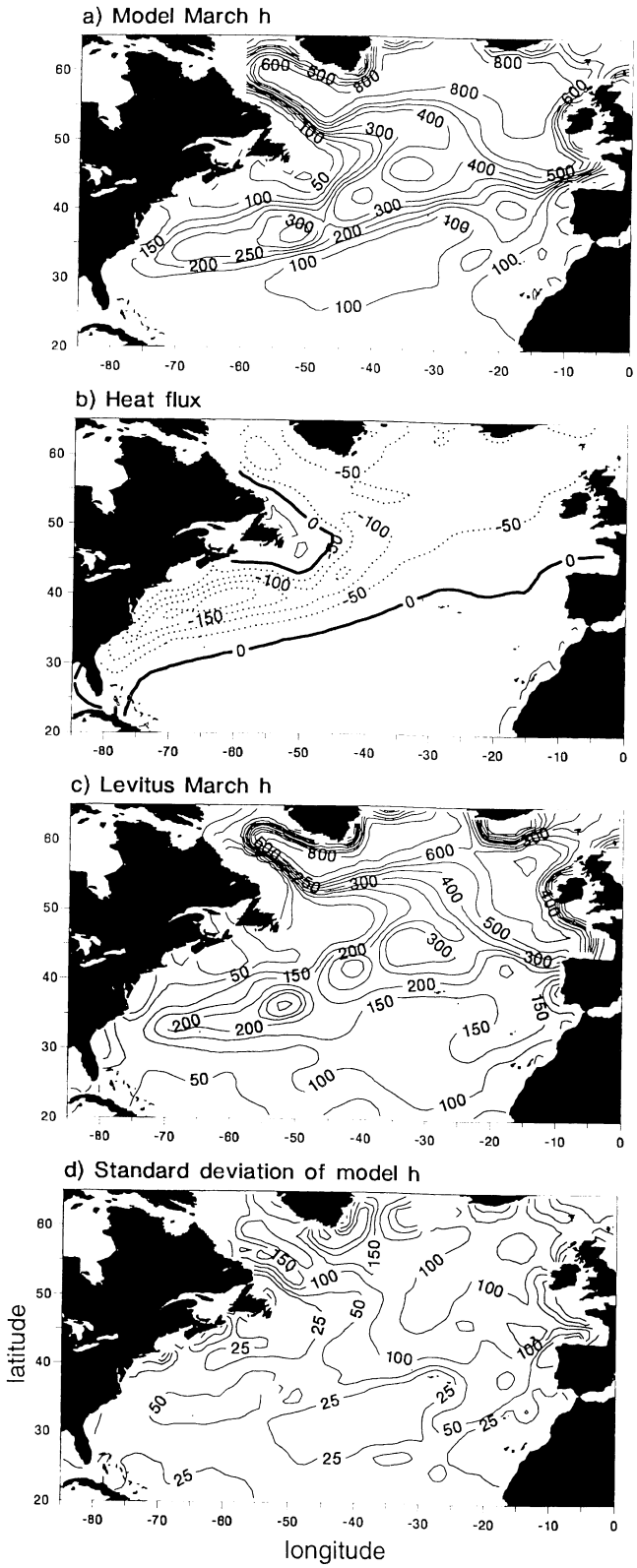

4.4. Interannual Variability of Convection

The variability in the surface heat and Ekman flux over winter (December-March), end of winter mixed-layer, and convective nitrate supply are shown in Figure 6 through a series of maps for all the pentads between 1968 and 1992. The variability in the heat flux over winter drives the modeled variability in the end of winter mixed-layer thickness and convective flux of nitrate. The heat flux anomaly is positive (into the ocean) over the western Atlantic during 1968-1972, weakly positive over the central Atlantic at 45°N, 40°W during 1973-1977 and 1978-1982, then weakly negative in 1983-1987 and strongly negative in 1988-1992 (Figure 6a).

Positive heat flux anomalies lead to thinner mixed layers. For example, the mixed layer is thinner over the western Atlantic and thicker over the eastern Atlantic during 1968-1972, while the reverse pattern occurs in 1988-1992 (Figure 6b). Accordingly, there is a reduced convective supply of nitrate whenever the mixed layer is thinner. In turn, the convective supply is weaker over the western Atlantic and stronger over the eastern Atlantic during 1968-1972, while the reverse occurs in 1988-1992 (Figure 6c). While the zero lines of mixed-layer thickness and convective flux anomaly are generally coincident, their gradients differ since the convective flux is also modulated by the vertical gradient of nitrate in the thermocline. Generally, the thickness anomalies are significantly greater at high latitudes compared to the subtropics. In contrast, the convective flux anomalies are comparable at mid-latitudes and high-latitudes owing to the poleward weakening of the nitrate gradient beneath the mixed layer.

4.5. Connection With the North Atlantic Oscillation

The dominant mode of atmospheric variability over the North Atlantic is associated with the North Atlantic Oscillation [*Hurrell*, 1995], where the NAO index is defined in terms of a sea-level pressure difference between Iceland and Portugal. A high NAO index correlates with enhanced winter surface heat loss and deep convective mixing in the subpolar gyre and Labrador Sea. The opposite is true during periods of low NAO index, with anomalous surface heat loss and enhanced convection in the subtropical gyre [*Dickson et al.*, 1996]. Con-

Figure 4. Mixed-layer thickness in March and annual heat flux: (a) model-derived, mixed-layer thickness (m) from an average of model output from 1968 to 1993; (b) diagnosed annual surface and Ekman heat flux (W m^{-2}); (c) data-derived, mixed-layer thickness (m) from climatological density profiles; and (d) standard deviation in the model-derived mixed-layer thickness (m) in March between 1968 and 1993.

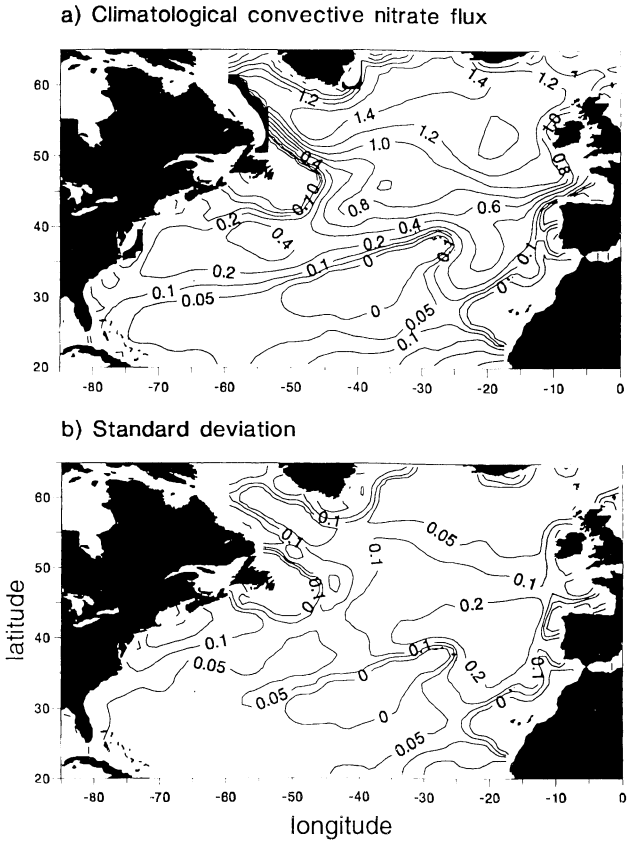

Figure 5. Model-derived convective flux of nitrate into the euphotic zone (mol N $m^{-2}yr^{-1}$) for the period from 1968 to 1993: (a) annual-mean contribution and (b) standard deviation in annual contributions.

sequently, we expect a similar relationship to occur for the winter entrainment of nutrients into the euphotic zone.

The correlation coefficients between the NAO index and modeled convective flux are shown in Figure 7. There are three regions of high correlation above a magnitude of 0.4, which is statistically significant to a level of 97.5%: in the subpolar gyre (55°N, 45°W) and southern and western parts of the subtropical gyres (25°N, 45°W and 35°N, 70°W). Elsewhere, there are extensive regions of weak correlation with the NAO index, particularly over the eastern Atlantic. The tripole pattern in the correlation coincides with the typical centers of change in sensible and latent heat flux associated with the NAO [*Cayan*, 1992a]. This pattern is to be expected since the modeled changes in winter convection are principally driven by changes in air-sea heat fluxes, rather than wind mixing or Ekman fluxes; in the mixed-layer model, wind mixing is only important during summer but not in winter.

Time series of the convective flux and the NAO index are shown over three $5° \times 5°$ regions over the North Atlantic (Figure 8), which include two of the regions of most significant correlation (Figure 7). Over the central subpolar gyre (e.g., 58°N, 43°W), the convective supply varies from 0.6 mol N $m^{-2}yr^{-1}$ to 1.4 mol N $m^{-2}yr^{-1}$ and has a strong positive correlation with the NAO index with a correlation coefficient of 0.76 (Figure 8a). In the western subtropical gyre (e.g., 28°N, 73°W), there are weaker variations from 0.01 mol N $m^{-2}yr^{-1}$ to 0.1 mol N $m^{-2}yr^{-1}$, which have a strong negative correlation with the NAO index with a correlation coefficient of −0.59 (Figure 8b). In contrast, in the eastern subtropical gyre (e.g., 48°N, 18°W), there is still marked variability with the convective flux varying from 0.7 mol N $m^{-2}yr^{-1}$ to 1.3 mol N $m^{-2}yr^{-1}$, but the variability is not significantly correlated with the NAO index (with a correlation coefficient of only −0.10) (Figure 8c).

The important inference here is that while there is variability in the convective flux, only a part of this variability is significantly associated with shifts in the NAO index. For example, the previous correlation coefficients suggest that the NAO explains typically 58% of the variability over the central subpolar gyre and 35% over the western subtropical gyre, but only 1% over the eastern subtropical gyre. Accordingly, we would expect there to be a similar correlation between changes in the NAO index and export production over the western and central Atlantic but no significant correlation over the eastern Atlantic.

To give further insight into the variability, we show composite maps for NAO+ and NAO− states (Figure 9). The NAO years selected to makes these maps are the 5 individual years with either the highest or lowest index between 1968 to 1993: the NAO+ composite is an average of 1983, 1989, 1990, 1992, and 1993, and the NAO− composite is an average of 1968, 1969, 1970, 1977, and 1979. The difference plot for the surface heat input over winter (December-March) (Figure 9a) shows the expected cooling over the subpolar gyre and warming over the western subtropical gyre reaching a magnitude of 50 W m^{-2}; also see the analysis by *Cayan* [1992a]. This heat flux anomaly drives a March mixed-layer deepening of more than 100 m in the subpolar gyre and a shallowing of 50 m in the western and eastern subtropical gyre (Figure 9b). While the heat flux change is only weakly positive over the eastern subtropical gyre, there is a significant shallowing of the mixed layer there. The resulting convective supply of nitrate to the euphotic zone is enhanced by 0.1 mol N $m^{-2}yr^{-1}$ over the subpolar gyre and weakened by 0.1 mol N $m^{-2}yr^{-1}$ over the western and eastern sides of the subtropical gyre (Figure 9c).

4.6. Climatology and Interannual Variability of the Ekman Supply

The climatological influence of Ekman advection on new and export production was examined by *Williams*

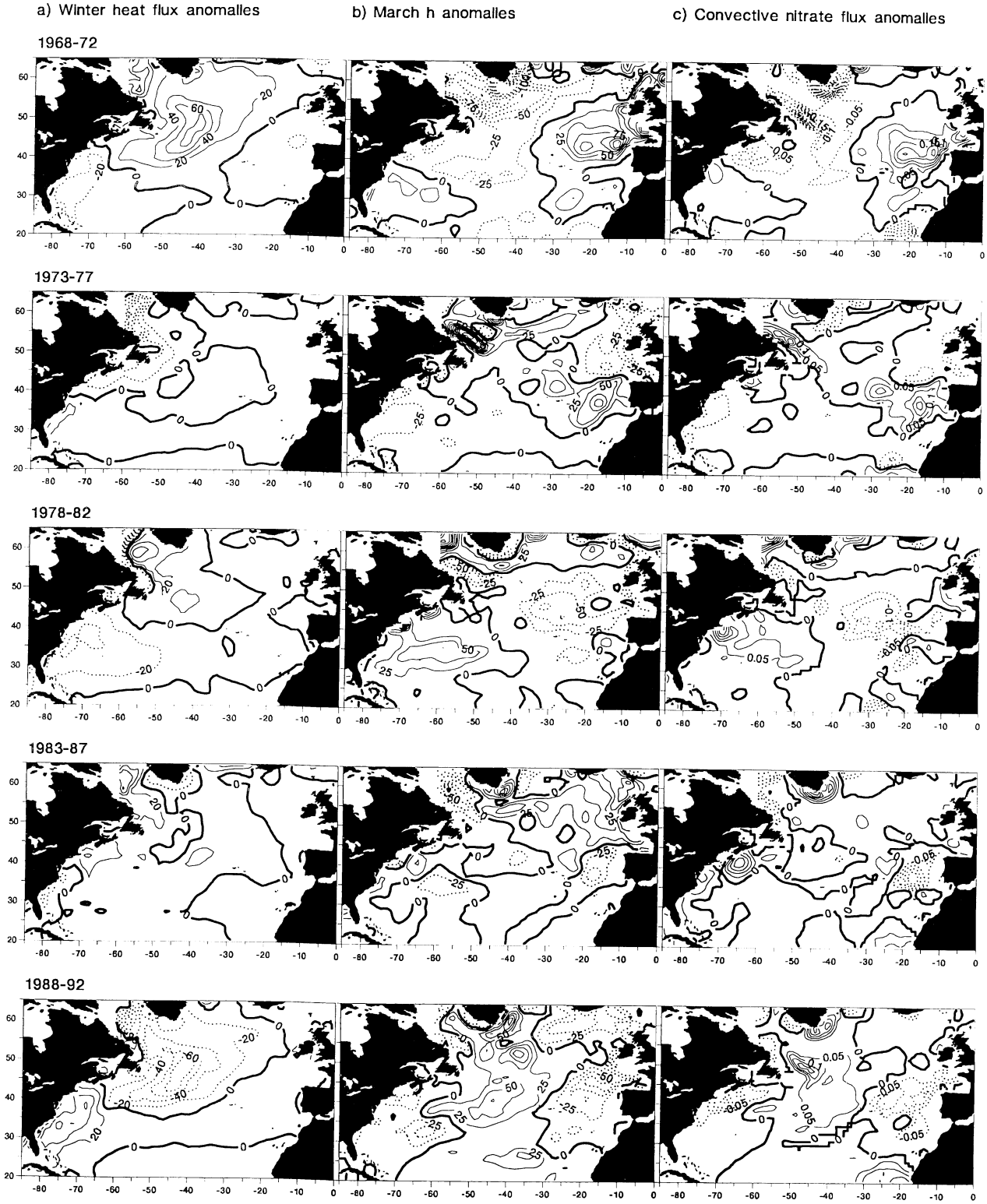

Figure 6. Pentad maps from 1968 to 1993 showing anomalies in (a) diagnosed surface and Ekman heat flux over winter (W m^{-2}), (b) model-derived, mixed-layer thickness (m) in March, and (c) model-derived, convective flux of nitrate into the euphotic zone (mol N $m^{-2}yr^{-1}$). These anomalies are relative to the climatological means shown in Figures 4b, 4a, and 5a.

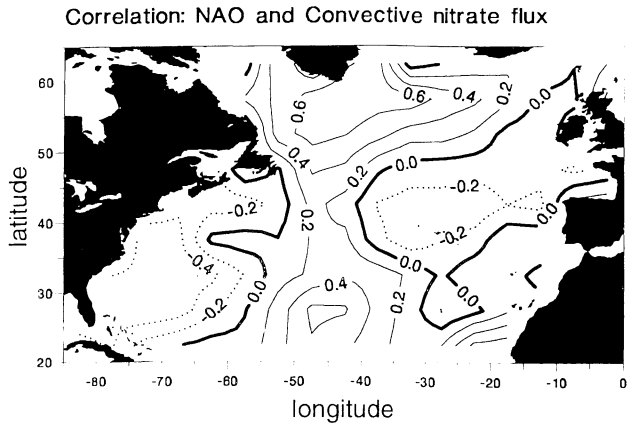

Figure 7. Map of the correlation coefficient between the model-derived, convective flux of nitrate and the North Atlantic Oscillation index [*Hurrell*, 1995]. Statistically significant values at a level of 97.5% have a correlation coefficient greater than 0.4 in magnitude.

and Follows [1998]. The Ekman circulation transfers nitrate to the euphotic zone via upwelling over the subpolar gyre and lateral transfer over the subtropical gyre (Figure 1b). The Ekman flux of nitrate is evaluated from the monthly contributions between September and April (when there is little biological activity) from 1968 to 1993 using the time series in wind stresses [*Kalnay et al.*, 1996] and our predicted nitrate concentrations in the mixed layer. The annual Ekman nitrate flux varies from 0.05 mol N $m^{-2}yr^{-1}$ in the subtropical gyre to 0.1 mol N $m^{-2}yr^{-1}$ over the subpolar gyre (Figure 10a). The standard deviation of the annual Ekman supply between 1968 and 1993 reaches 0.05 mol N $m^{-2}yr^{-1}$ over the subpolar gyre (Figure 10b). While this Ekman transfer is generally an order of magnitude smaller than the convective transfer, the Ekman supply makes a significant contribution in the intergyre region and is important in maintaining the nutrient budget of the seasonal boundary layer.

Here, we examine the interannual variations in the Ekman contribution. The North Atlantic storm track varies with stronger westerly winds in the NAO+ state and a weaker, westerly jet shifted to the south during the NAO− phase. These wind stress changes alter the vertical and horizontal Ekman nitrate supply in contrasting ways. The positive correlation between the Ekman supply and the NAO index around 50°N is due to enhanced horizontal Ekman transfer through both stronger winds and stronger meridional gradients in surface nitrate with enhanced convection in the subpolar gyre (Figure 10c). The negative correlation around 35°N is due to more extensive upwelling occurring with a southward shift of the westerly jet. However, the difference in the Ekman supply of nitrate between the composite of NAO+ and NAO− states is relatively small compared with the convective change, only reaching 0.1 mol N $m^{-2}yr^{-1}$ around 50°N, 45°W (Figure 10d).

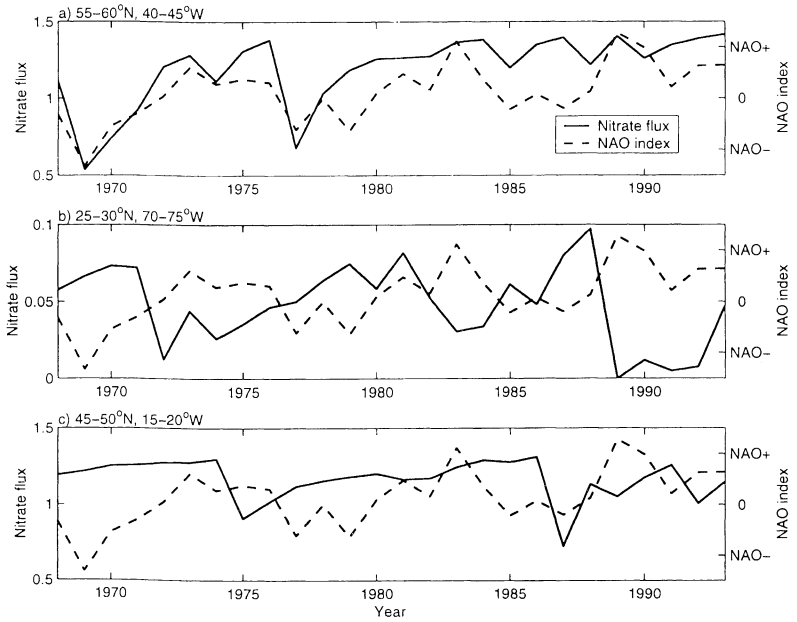

Figure 8. Time series for the model-derived, convective flux of nitrate (full line) together with the North Atlantic Oscillation index (dashed line): (a) subpolar gyre, 55-60°N, 40-45°W; (b) western subtropical gyre, 25-30°N, 70-75°W; (c) eastern subtropical gyre, 45-50°N, 15-20°W. The correlation coefficients between the time series and the NAO index are 0.76, −0.59, and −0.10, respectively.

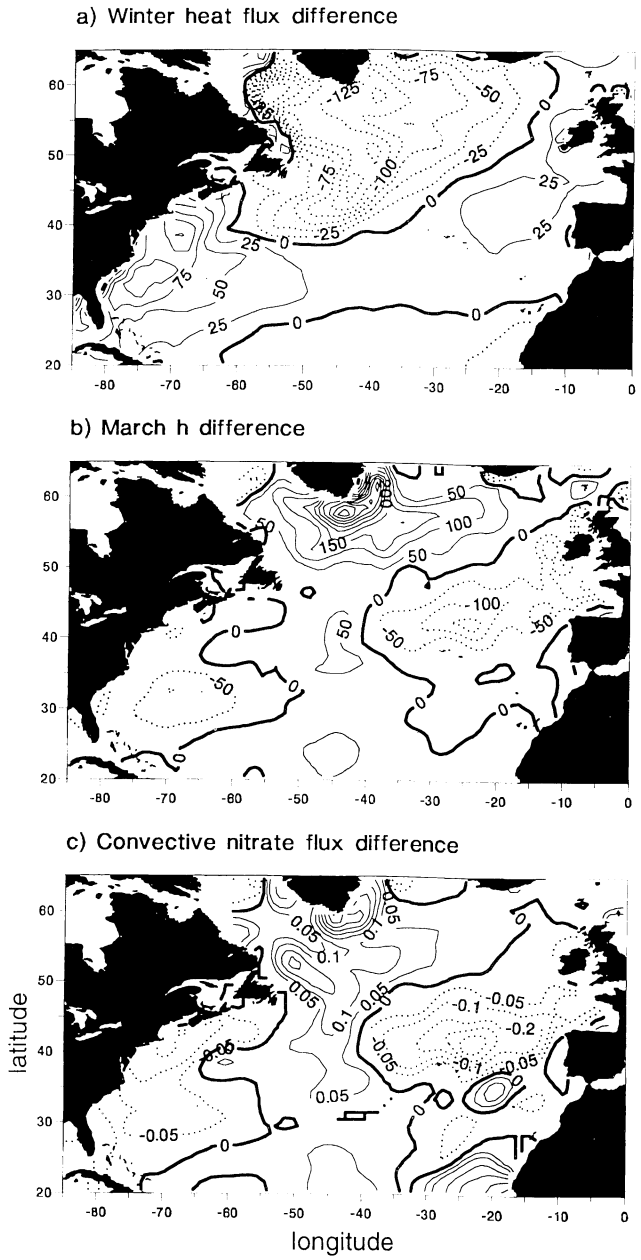

Figure 9. Difference plots between composite NAO+ and NAO− states for (a) diagnosed surface and Ekman heat flux (W m^{-2}) over winter, (b) model-derived, end of winter mixed-layer thickness (m), and (c) model-derived, convective flux of nitrate (mol N $m^{-2}yr^{-1}$).

Consequently, the convective supply to the euphotic zone dominates over the Ekman supply for both its climatological mean and variability. However, the Ekman supply is still important in the long-term maintenance of the nutrient concentrations over the seasonal boundary layer. The variability in the Ekman supply is more strongly correlated with the NAO index over a greater part of the North Atlantic basin than is the convective supply. This difference in correlation patterns is probably due to the NAO index being defined in terms of sea-level pressure difference, which is directly related to surface winds that drive Ekman fluxes but is less directly related to surface heat fluxes that drive convection.

5. Discussion

In this study, the convective and Ekman supplies of nitrate to the surface ocean are estimated over the North Atlantic, addressing both the climatological mean and interannual variations over a 26-year period. Our focus on the mean contribution and variability of nitrate transport does not account for other, potentially important, contributions in the supply of new nitrogen, such as nitrogen fixation, transport of dissolved organic matter, and eddy-rectified transport.

5.1. Climatological-Mean Supply of Nitrate

A matrix of one-dimensional, mixed-layer models is used to estimate the mixed-layer thickness from 1968 to 1993, forced by time series of surface and Ekman fluxes of heat and fresh water and including parameterized geostrophic advection. The convective and Ekman supply of nitrate to the euphotic zone is evaluated by combining the mixed-layer predictions with wind stresses and climatological nitrate profiles. There is a general poleward increase in convective supply from 0.1 mol N $m^{-2}yr^{-1}$ in the subtropics to 1.4 mol N $m^{-2}yr^{-1}$ over the subpolar gyre. The climatological, annual-mean Ekman transfer is relatively small, reaching 0.1 mol N $m^{-2}yr^{-1}$ over the subpolar gyre but is important in maintaining nitrate concentrations within the seasonal boundary layer. The details of the model predictions should be viewed with some caution due to a number of significant uncertainties in our approach. The air-sea fluxes used to force the model have errors of typically ± 25 W m^{-2}, which is comparable to the climatological mean over much of the basin. The model neglects changes in the geostrophic flow on timescales shorter than 10 years. The convective nitrate supply might also be over estimated in instances where there is repeated annual deepening of the winter mixed-layer, since the model assumes that the nitrate profile in the main thermocline is always maintained. However, despite these uncertainties, the resulting maps of the annual convective nitrate supply have a plausible basin-scale structure.

The convective flux into the euphotic zone will eventually diminish (over a period of several years) unless there is some other process fluxing nutrients into the seasonal boundary layer. Over the subpolar gyre, the wind-induced upwelling and cyclonic circulation generally transfer nutrients from the thermocline into the seasonal boundary layer, which thickens poleward. Over the subtropical gyre, the horizontal Ekman and eddy

transport is important in providing nutrients to the euphotic zone on the flanks of the gyre and across frontal zones, such as the Gulf Stream and Azores Current. Over the central part of the subtropical gyre, convection or the gyre transport is too weak to explain the levels of export production. Instead, these processes have to be augmented by other physical transfers, such as rectified eddy upwelling and lateral influx of dissolved organic nutrients, or other atmospheric sources, such as nitrogen fixation.

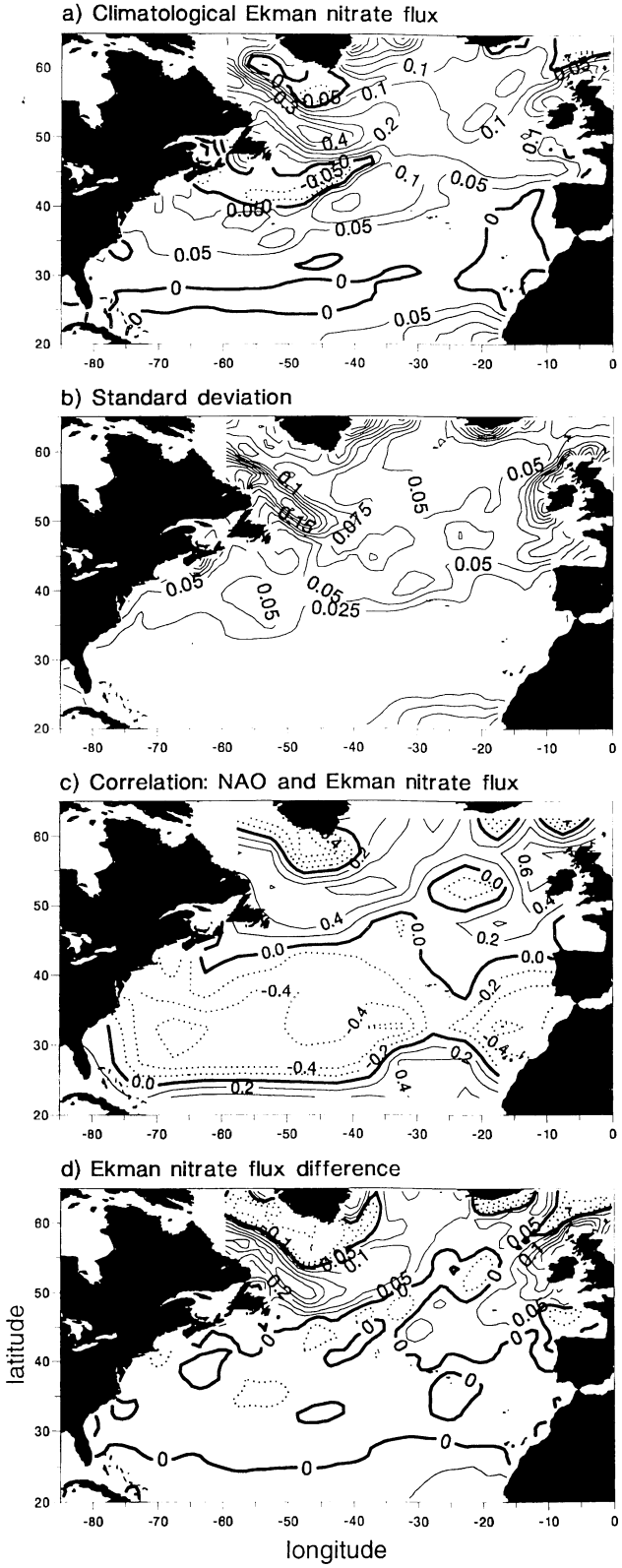

5.2. Interannual Variations in the Nitrate Supply

Our study assumes that atmospheric anomalies drive the interannual variability on the basin scale over the upper ocean. Over a period of 26 years, the model suggests that the interannual variability in the nitrate supply reaches ± 0.2 mol N $m^{-2}yr^{-1}$ in the eastern Atlantic. The interannual variability in nitrate supply is largely controlled by convection rather than Ekman transfer. The convective variability is only significantly correlated with the NAO between parts of the western and central Atlantic but not the eastern Atlantic. Instead, there is significant convective variability controlled by the local heat loss to the overlying atmosphere, rather than the basin-scale measure provided by NAO. The Ekman transfer of nitrate shows a stronger correlation with the NAO over much of the subtropical gyre with enhanced nitrate supply occurring when the westerly jet shifts southward during a NAO− state.

Expressed in terms of equivalent carbon fluxes, the area-averaged convective flux of nitrate from 20°N to 65°N is equivalent to a carbon flux of 1.1 Gt C yr^{-1} assuming a Redfield ratio of C:N = 105:15. The standard deviation in this carbon flux is 0.13 Gt C yr^{-1}. However, we do not expect the variability in the convective flux of nitrate significantly to impact on the atmospheric uptake of carbon dioxide, since the nitrate flux will be accompanied by a carbon flux in approximate Redfield ratio (through the biological control of the vertical gradients in carbon and nitrogen).

Interannual changes in the ecosystem may be statistically correlated with the state of the atmosphere. For example, in situ observations of plankton species in the

Figure 10. Maps of Ekman nitrate flux (mol N $m^{-2}yr^{-1}$) into the euphotic zone for (a) model-derived, annual flux between 1968 and 1993, (b) standard deviation in the annual flux between 1968 and 1993, (c) correlation coefficient between the annual flux between 1968 and 1993 with the NAO index with statistically significant values at a level of 97.5% having a value greater than 0.4, and (d) difference map for the model-derived, Ekman nitrate flux between composite NAO+ and NAO− states.

North Atlantic appear to correlate with indicators of regional climate patterns related to the NAO index [*Taylor and Stephens*, 1980; *Aebischer et al.*, 1990]. However, the significance of the NAO index and any statistical correlations might be unreliable due to the short length of the time record [*Wunsch*, 1999].

The causal mechanisms connecting the detailed ecosystem response to the atmosphere have yet to be identified. In our view, such connections might, in part, be stimulated in nutrient-limited areas by meteorological modulation of oceanic convection and circulation altering, in turn, the nutrient supply to the euphotic zone. In nutrient replete, light-limited areas, interannual changes in convection also impinge on the ecosystem by modifying the light experienced by biota during the spring [*Dutkiewicz et al.*, 2000] and, possibly, the winter survival rate of zooplankton and their subsequent grazing of phytoplankton [*Fasham*, 1995].

Acknowledgments. A.M. is grateful for support from a NERC studentship GT4/95/163/M and from the James Rennell Division of the Southampton Oceanography Centre. A.M. would also like to thank Plymouth Marine Laboratory for providing facilities to allow her to work there. M.J.F. is grateful for support from NASA, grant NCC5-244. We would like to acknowledge the importance of the time series programs at BATS and Hydrostation S.

References

Aebischer, N.J., J.C. Coulson, and J.M. Colebrook, Parallel long-term trends across four marine trophic levels and weather, *Nature, 347*, 753–755, 1990.

Battisti, D.S., U.S. Bhatt, and M.A. Alexander, A modelling study of the interannual variability in the wintertime North Atlantic Ocean, *J. Clim., 8*, 3067–3083, 1995.

Behrenfeld, M.J., and P.G. Falkowski, Photosynthetic rates derived from satellite-based chlorophyll concentration, *Limnol. Oceanogr., 42*, 1–20, 1997.

Bjerknes, J., Atlantic air-sea interaction, *Adv. Geophys., 20*, 1–82, 1964.

Cayan, D.R., Latent and sensible heat flux anomalies over the northern oceans: The connection to monthly atmospheric circulation, *J. Clim., 5*, 354–369, 1992a.

Cayan, D.R., Latent and sensible heat flux anomalies over the Northern Oceans: Driving the sea surface temperature, *J. Phys. Oceanogr., 22*, 859–881, 1992b.

Conkright, M.E., S. Levitus, and T.P. Boyer, *World Ocean Atlas 1994*, vol. 1, *Nutrients*, 150 pp., U.S. Dep. of Commer., Natl. Oceanic and Atmos. Admin., Washington D.C., 1994.

da Silva A.M., C.C. Young, and S. Levitus, *Atlas of Surface Marine Data 1994*, vol. 1, *Algorithms and Procedures*, U.S. Dep. of Commer., Natl. Oceanic and Atmos. Admin., Washington D.C., 1994.

Dickson, R., On the relationship between ocean transparency and the depth of the sonic scattering layers in the North Atlantic, *J. Cons. Int. Explor. Mer., 34*(3), 416–422, 1972.

Dickson, R., J. Lazier, J. Meinke, P. Rhines, and J. Swift, Long term coordinated changes in the convective activity of the North Atlantic, *Prog. Oceanogr., 38*, 241–295, 1996.

Doney, S. C., A synoptic atmospheric surface forcing data set and physical upper ocean model for the U.S. JGOFS Bermuda Atlantic Time-Series Study site, *J. Geophys. Res., 101*, 25,615–25,634, 1996.

Dutkiewicz, S., M. Follows, J. Marshall, and W.W. Gregg, Interannual variability of phytoplankton abundances in the North Atlantic, *Deep Sea Res.*, in press, 2000.

Fasham, M.J.R., Variations in the seasonal cycle of biological production in subarctic oceans: A model sensitivity analysis, *Deep Sea Res., Part I, 42*, 1111–1149, 1995.

Glover, D.M., and P.G. Brewer, Estimates of wintertime mixed layer nutrient concentrations in the North Atlantic, *Deep Sea Res., 35*, 1525–1546, 1988.

Gruber, N., and J.L. Sarmiento, Global patterns of marine nitrogen fixation and denitrification, *Global Biogeochem. Cycles, 11*, 235–266, 1997.

Horch, A., W. Barkmann, and J.D. Woods, Die Erwärmung des Ozeans hervogerufen durch solare Strahlungsenergie, *Nr 120*, Berichte aus dem Institut für Meereskunde and der Universität Kiel, Kiel, Germany, 1983.

Hurrell, J.W., Decadal trends in the North Atlantic Oscillation: Regional temperatures and precipitation, *Science, 269*, 676–679, 1995.

Jenkins, W.J., Oxygen utilization rates in North Atlantic subtropical gyre and primary production in oligotrophic systems, *Nature, 300*, 246–248, 1982.

Jenkins, W.J., Nitrate flux into the photic zone near Bermuda, *Nature, 331*, 521–523, 1988.

Jenkins, W.J., and J.C. Goldman, Seasonal oxygen cycling and primary production in the Sargasso Sea, *J. Mar. Res., 43*, 465–491, 1985.

Kalnay, E., et al., The NCEP/NCAR 40-year reanalysis project, *Bull. Am. Meteorol. Soc., 77*, 437–471, 1996.

Knap, A., T. Jickells, A. Pszenny, and J. Galloway, Significance of atmospheric-derived fixed nitrogen on productivity of the Sargasso Sea, *Nature, 320*, 158–160, 1986.

Kraus, E.B., and J.S. Turner, A one-dimensional model of the seasonal thermocline, II, The general theory and its consequences, *Tellus, 19*, 19–105, 1967.

Kushnir, Y., Interdecadal variations in North Atlantic sea surface temperature and associated atmospheric conditions, *J. Clim., 7*, 141–157, 1994.

Lampitt, R.S., and A.N. Antia, Particle flux in deep seas: regional characteristics and temporal variability, *Deep Sea Res., 44*, 1377–1403, 1997.

Lascaratos, A., R.G. Williams, and E. Tragou, A mixed-layer study of the formation of Levantine Intermediate Water, *J. Geophys. Res., 98*, 14,739–14,747, 1993.

Levitus, S., and T. P. Boyer, *World Ocean Atlas 1994*, vol. 4, *Temperature*, U.S. Dep. of Commer., Nat. Oceanic and Atmos. Admin., Washington D. C., 1994.

Levitus, S., R. Burgett, and T. P. Boyer, *World Ocean Atlas 1994*, vol. 3, *Salinity*, U.S. Dep. of Commer., Nat. Oceanic and Atmos. Admin., Washington D. C., 1994.

Lewis, M.R., W.G. Harrison, N.S. Oakley, D. Hebert, and T. Platt, Vertical nitrate fluxes in the oligotrophic ocean, *Science, 234*, 870–873, 1986.

Marshall, J.C., A.J.G. Nurser, and R.G. Williams, Inferring the subduction rate and period over the North Atlantic, *J. Phys. Oceanogr., 23*, 1315–1329, 1993.

McGillicuddy, D.J., and A.R. Robinson, Eddy-induced nutrient supply and new production in the Sargasso Sea, *Deep Sea Res., Part I, 44*, 1427–1449, 1997.

McGillicuddy, D.J., A.R. Robinson, D.A. Siegel, H.W. Jannasch, R. Johnson, T. Dickeys, J. McNeil, A.F. Michaels, and A.H. Knap, New evidence for the impact of mesoscale

eddies on biogeochemical cycling in the Sargasso Sea, *Nature, 394*, 263–266, 1998.

McKinley, G., M.J. Follows, and J.C. Marshall, Interannual variability in air-sea fluxes of oxygen in the North Atlantic, *Geophys. Res. Lett.*, in press, 2000.

Menzel, D.W., and J.H. Ryther, Annual variations in primary production in the Sargasso Sea off Bermuda, *Deep Sea Res., 7*, 282–288, 1961.

Michaels, A.F., and A.H. Knap, Overview of the U.S. JGOFS Bermuda Atlantic Time-series Study and of the Hydrostation S program, *Deep Sea Res., Part II, 43*, 157–198, 1996.

Michaels, A.F., et al., Seasonal patterns of ocean biogeochemistry at the U.S. JGOFS Bermuda Atlantic Time-series Study site, *Deep Sea Res., Part I., 41*, 1013–1038, 1994.

Michaels, A.F., D. Olson, J.L. Sarmiento, J.W. Ammerman, K. Fanning, R. Jahnke, A.H. Knap, F. Lipschultz, and J.M. Prospero, Inputs, losses and transformations of nitrogen and phosphorus in the pelagic North Atlantic Ocean, *Biogeochemistry, 35*, 181–226, 1996.

Oschlies, A., and V. Garcon, Eddy-induced enhancement of primary production in a model of the North Atlantic Ocean, *Nature, 394*, 266-269, 1998.

Payne, R.E., Albedo of the sea surface, *J. Atmos. Sci., 29*, 959–970, 1972.

Reynolds, R.W., and T.M.Smith, Improved global sea surface temperature analyses, *J. Clim., 7*, 929–948, 1994.

Rintoul, S.R., and C. Wunsch, Mass, heat, oxygen and nutrient fluxes and budgets in the North Atlantic Ocean, *Deep Sea Res., Part I, 38*, S355–S377, 1991.

Sathyendranath, S., R.S.A. Longhurst, C.M. Caverhill, and T. Platt, Regionally and seasonally differentiated primary production in the North Atlantic, *Deep Sea Res., 42*, 1773–1802, 1995.

Steele, J.H., and E.W. Henderson, "The Significance of Interannual Variability" in *Towards a Model of Ocean Biogeochemical Variability,* edited by G.T. Evans and M.J.R. Fasham, pp. 237–260, Springer–Verlag, New York, 1993.

Taylor, A.H., and J.A. Stephens, Latitudinal displacements of the Gulf Stream (1966 to 1977)and their relation to changes in temperature and zooplankton abundance in the N.E. Atlantic, *Oceanol. Acta, 3*, 145–149, 1980.

Williams, R.G., Modification of ocean eddies by air-sea interaction, *J. Geophys. Res., 93*, 15,523–15,533, 1988.

Williams, R.G., and M.J. Follows, The Ekman transfer of nutrients and maintenance of new production over the North Atlantic, *Deep Sea Res., Part I, 45*, 461–489, 1998.

Wunsch, C., The interpretation of short climate records, with comments on the North Atlantic and Southern Oscillations, *Bull. Am. Meteorol. Soc., 80*, 245–255, 1999.

M. J. Follows, Program in Atmospheres, Oceans and Climate, Massachusetts Institute of Technology, Cambridge, MA 02139. (e-mail: mick@plume.mit.edu)

A. J. McLaren and R. G. Williams, Oceanography Laboratories, Department of Earth Sciences, University of Liverpool, Beford Street North, Liverpool, L69 7ZL, UK. (e-mail: A.Mclaren@liv.ac.uk; ric@liv.ac.uk)

(Received January 12, 2000; revised June 13, 2000; accepted August 7, 2000.)